RESEARCH PAPER

Stability of Double-Diffusive Shear Flow in Inclined Cavities

Mohana Priya. M[1], Rohith Roshan. A[2] and Sumathi. K[3]

[1,3]*Department of Mathematics, PSGR Krishnammal College for Women, Coimbatore-641 004*
[2]*Department of Mechanical Engineering, College of Engineering, Guindy Campus, Anna University, Chennai- 600 025*

ABSTRACT
This paper presents a comprehensive stability analysis of a fluid system by examining the governing equations for velocity, temperature, and concentration. By using dimensionless parameters such as the Prandtl (*Pr*), Schmidt (*Sc*), and Grashof (*Gr*) numbers, this study deals with fundamental equations with boundary conditions at $x = \pm 1$. The core of the analysis involves introducing a perturbed state and deriving linearized equations to assess the system's response to disturbances. By applying a perturbation expansion method where variables are expressed as power series in terms of the wave number *k*, the research systematically solves for the zeroth-order and first-order stability components. The mathematical derivation culminates in determining the growth rate (σ) through characteristic equations and hyperbolic function solutions, providing a framework to characterize the stability of the fluid flow.
Keywords: *Stability, Inclined cavity, Prandtl number (Pr), Schmidt number (Sc), Grashof number (Gr), wave number (k)*
How to cite this article: Mohana Priya. M, Rohith Roshan. A and Sumathi. K, Stability of Double-Diffusive Shear Flow in Inclined Cavities. Int J Drug Deliv Technol. 2026;16(16s): 506-516. DOI: 10.25258/ijddt.16.16s.54
Source of support: Nil.
Conflict of interest: None

1. INTRODUCTION

In fluid mechanics, stability refers to how well a flow state can resist changes. A base state, which is usually calm and diffusive, may become unstable if a control parameter, like the Rayleigh number (Ra), surpasses a critical point.

Double-diffusive convection is fluid motion caused by gradients of two or more diffusing properties with different molecular diffusivities. A common example is a fluid layered by both temperature and solute concentration, such as salt. Temperature diffuses quickly, while solute concentration diffuses slowly, resulting in interesting phenomena like layered convection, fingering instabilities, and oscillatory flows. These processes are essential in fields like oceanography, geology, material science, and engineering.

When this system is confined in an enclosure and tilted with respect to gravity, the situation becomes much more complex. The tilt links the buoyancy forces to the shape of the cavity, creating a rich structure of bifurcations, multiple steady states, and complex paths to instability and chaos. Therefore, the stability of double-diffusive flow in inclined cavities is a key issue in fluid dynamics with important real-world implications.

Gill(1966) examined the stability of double-diffusive flow in a vertical slot and he worked that a parallel flow solution exists for tall cavities. When buoyancy forces oppose each other, the flow can become unstable to traveling waves.

Lee and Korpela (1983) examined a linear stability analysis for a vertical cavity with opposing temperature and concentration gradients. They identified oscillatory instabilities and they revealed that the critical Rayleigh number for the onset of oscillatory convection decreases as the Lewis number (Le) increases. In a horizontal layer heated from below, similar to the Rayleigh-Bénard configuration, and with a stabilizing solute gradient, the issue becomes similar to thermohaline convection.

Nield (1967) studied the linear stability analysis and demonstrated that the system can lose its stability for both stationary and oscillatory modes, Le and N-dependent. Veronis (1968) found that the presence of a stabilizing solute gradient prevents convection in a fluid subject to an adverse temperature gradient. Instability may occur in the form of oscillations because of the stabilizing effect of solute.

Shivakumara *et al* (1985) expanded linear theory for rotating double-diffusive layers. They predicted new stability boundaries for salt-finger and diffusive convection. Their weakly nonlinear analysis, which used a truncated Fourier series, illustrated that heat and mass transport increase with the Rayleigh number but decrease with the Prandtl number, diffusivity ratio, and Taylor number.

Sarkar and Phillips (1992) applied linear stability analysis to examine thermohaline instabilities in infinite porous media. They found that the reference state is always unstable to salt fingers for positive vertical Rayleigh numbers and interleaving for negative values. Woods and Linz [1996] analytically demonstrated that tilting a fluid-filled fracture from the vertical inevitably generates convective flow, even under a stable temperature gradient. Buscalioni and Crespo del Arco (1999) examined the primary and secondary flow within an inclined cavity. According to the results of their linear stability analysis, stationary or oscillatory instabilities can break down basic unicellular motion.

**Author for Correspondence: Mohana Priya. M*

Sharifi and Rasouli (2024) focuses specifically on confined geometries, systematically analyzing heat and mass transfer progress within enclosures such as rectangular, square, and annular cavities under various thermal and solutal boundary conditions. Again, Sharifi and Rasouli (2025) examining the influence of external forces—including magnetic fields, rotation, and vibration-alongside the effects of complex flow geometries and porous media.

2 FLOW DESCRIPTION AND GOVERNING EQUATIONS

The flow system is a double-diffusive convection model in an inclined channel. It's governed by the conservation of mass, momentum, energy, and species concentration, with flow driven by thermal and solutal buoyancy forces represented by the Grashof (Gr) and modified Grashof (Gm) numbers. In its steady state, the fluid flows parallel to the walls with a velocity $w_0(x)$ and maintains linear temperature and concentration gradients vertically. To evaluate the stability of this setup, small perturbations are introduced and linearized. The stream function (ϕ) and growth rate (σ) are expressed as power series of the wave number k.

Below is a diagram that illustrated the fundamental flow and geometry of problem.

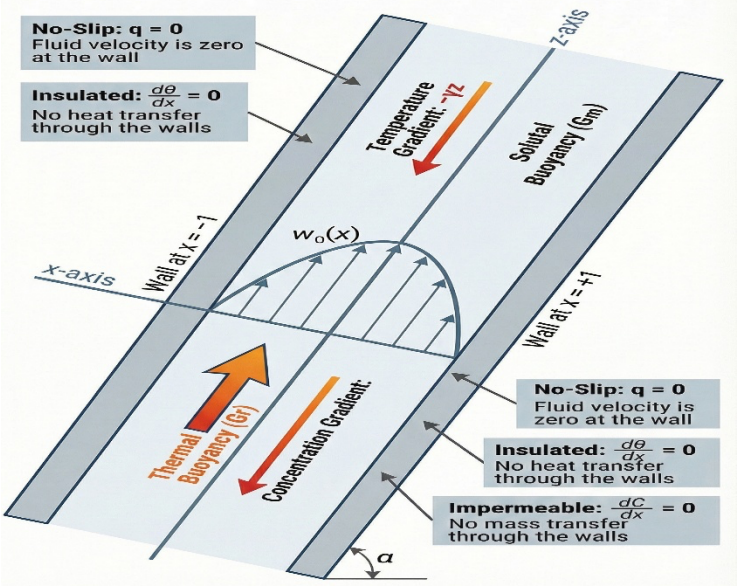

Figure 1: Schematic diagram

In the present work, the following assumptions are made:

- The Newtonian flow, which is laminar and inviscid is taken into consideration.
- The cavity is tilted α degrees with respect to gravity and filled with an incompressible viscous fluid.
- The non-slip boundary condition is used at the boundaries and the temperature in the walls x= ±1
- In the momentum equation, the Boussinesq approximation is being used.
- Double-diffusive natural convection is taken into consideration.
- Only two-dimensional disturbances are taken into consideration.

The equations governing the motion with the Boussinesq approximation are given below

$$\nabla \cdot \vec{q}' = 0 \tag{1}$$

$$\rho_0 \left[\frac{\partial \vec{q}'}{\partial t'} + (\vec{q}' \cdot \nabla)\vec{q}'\right] = -\nabla p' + \rho' g \hat{e}_g \tag{2}$$

$$\frac{\partial T'}{\partial t'} + (\vec{q}' \cdot \nabla')T' = k\nabla'^2 T' \tag{3}$$

$$\frac{\partial C'}{\partial t'} + (\vec{q}' \cdot \nabla')C' = D\nabla'^2 C' \tag{4}$$

$$\rho' = \rho_0\left(1 - \beta_T^*(T' - T_0) - \beta_M^*(C' - C_0)\right) \tag{5}$$

By introducing the non-dimensionlisation parameters

$$(x', y', z') = h(x, y, z); t' = \frac{h^2}{\vartheta} t \quad ;$$

$$(u', v', w') = \frac{\nu}{h}(u, v, w); \quad \vec{q}' = \frac{\nu}{h}\vec{q}; \quad p = \frac{\rho_0 \nu^2}{h^2};$$

$$\theta = \frac{(T' - T_0)}{(T_W - T_0)}; \qquad C = \frac{(C' - C_0)}{(C_W - C_0)};$$

$$T' = T_0 + (T_W - T_0)\cdot\theta$$

;

$$C' = C_0 + (C_W - C_0)\cdot C$$

in equations (1) to (5), we get the governing equations in non-dimensional form as follows:

$$\nabla\cdot\vec{q} = 0 \tag{6}$$

$$\frac{\partial\vec{q}}{\partial t} + (\vec{q}.\nabla)\vec{q} = -\nabla p + (Gr\,\theta - Gm\,C)(\sin\alpha\,\hat{\imath} - \cos\alpha\,\hat{k}) \tag{7}$$

$$\frac{\partial\theta}{\partial t} + (\vec{q}.\nabla)\theta = \frac{1}{Pr}\nabla^2\theta \tag{8}$$

$$\frac{\partial C}{\partial t} + (\vec{q}.\nabla)C = \frac{1}{Sc}\nabla^2 C \tag{9}$$

Where, the Prandtl number, Schmidt number and Grashof number for mass transfer are defined respectively as Pr= ν/k, Sc= ν/D, $Gr = \frac{g\beta_T(T_W-T_0)h^3}{\nu^2}$ and $Gm = \frac{g\beta_c(C_W-C_0)h^3}{\nu^2}$.

We impose the no-slip boundary conditions at all rigid boundaries and the temperature at the walls $x = \pm 1$ satisfies the homogeneous heat conduction equation.

$$\vec{q} = 0, \frac{\partial\theta}{\partial t} = 0, \frac{\partial C}{\partial t} = 0 \text{ at } x = \pm 1 \tag{10}$$

At equilibrium, we have assumed the basic velocity, temperature and concentration profiles as follows

$$\vec{q} = (0,0,w_0(x))$$
$$\theta = -\eta z + b + \theta_0(x) \tag{12}$$
$$C = -\eta_c z + b_c + C_0(x)$$

Hence the equilibrium state flow profiles are governed by the following equations

$$Gr\,cos\alpha\theta_0'(x) + Gm\,sin\alpha C_0'(x) = Gr\,\eta\,sin\alpha + Gm\eta_c sin\alpha$$

$$\frac{\partial^2\theta_0}{\partial x^2} + \mathrm{Pr}\,\eta\,w_0(x) = 0$$

$$\frac{\partial^2 C_0}{\partial x^2} + \mathrm{Sc}\,\eta_c\,w_0(x) = 0$$

In order to study the stability of the basic flow, we proceed in the usual form. The flow variables are written as the sum of the mean flow quantity and a small perturbation.

The stream function of the perturbation flow satisfies $u = ik\varphi$, $w = -\frac{\partial\varphi}{\partial x}$.

Hence the governing equations for perturbed state are given by

$$-\sigma\left(\frac{\partial^2}{\partial x^2} - k^2\right)\varphi - ikw_0\left(\frac{\partial^2}{\partial x^2} - k^2\right)\varphi + ikw_0''\varphi - Gr(iksin\,\alpha\,\theta + \cos\alpha\,\theta') - Gm\,(iksin\,\alpha\,C + \cos\alpha\,C') = 0 \tag{17}$$

$$Pr^{-1}\left(\frac{\partial^2}{\partial x^2} - k^2\right)\theta - \sigma\theta - ik(\varphi\theta'_0 + w_0\theta) - \eta\varphi' = 0 \tag{18}$$

$$Sc^{-1}\left(\frac{\partial^2}{\partial x^2} - k^2\right)C - \sigma C - ik(\varphi C'_0 + w_0 C) - \eta_C\varphi' = 0 \tag{19}$$

With boundary conditions, $\varphi(\pm1) = \varphi'(\pm1) = \theta_0'(\pm1) = C_0'(\pm1) = 0$

(20)

Equations (17) - (20) have non-trivial solutions only for certain values of the frequency parameter σ (eigen values). The boundary value problem is not self-adjoint. Hence in general the frequency of the disturbances σ will admit complex values which will determine the stability of the problem.

3 STABILITY ANALYSIS

In this section we analyse the behaviour of the disturbances for long waves i.e., k is assumed to be small. We attempt to find analytical expressions for the growth rate and stream using regular perturbation method. Assuming

$$\sigma = \sigma_0 + k\sigma_1 + k^2\sigma_2 + \cdots$$
$$\varphi = \varphi_0 + k\varphi_1 + k^2\varphi_2 + \cdots$$
$$\theta = T_0 + kT_1 + k^2T_2 + \cdots$$
$$C = F_0 + kF_1 + k^2F_2 + \cdots \tag{11}$$
(21)

Substituting (21) in (17) – (20), we get

$$-(\sigma_0 + k\sigma_1 + k^2\sigma_2 + \cdots)\left(\frac{\partial^2}{\partial x^2} - k^2\right)(\varphi_0 + k\varphi_1 + k^2\varphi_2 + \cdots) \tag{13}$$

$$-ik\,w_0(x)\left(\frac{\partial^2}{\partial x^2} - k^2\right)(\varphi_0 + k\varphi_1 + k^2\varphi_2 + \cdots) \tag{14}$$

$$+ikw_0''(x)(\varphi_0 + k\varphi_1 + k^2\varphi_2 + \cdots) \tag{15}$$

$$-Gr(ik\sin\alpha)(T_0 + kT_1 + k^2T + \cdots) \tag{16}$$

$$-Gr(\cos\alpha)(T'_0 + kT'_1 + k^2T'_2 + \cdots)$$

$$-Gm(ik\sin\alpha)(F_0 + kF_1 + k^2F_2 + \cdots)$$

$$-Gm(\cos\alpha)\,(F'_0 + kF'_1 + k^2F'_2 + \cdots) = 0 \tag{22}$$

$$Pr^{-1}\left(\frac{\partial^2}{\partial x^2} - k^2\right)(T_0 + kT_1 + k^2T_2 + \cdots)$$

$$-(\sigma_0 + k\sigma_1 + k^2\sigma_2 + \cdots)(T_0 + kT_1 + k^2T_2 + \cdots)$$

$$-ik(\,\varphi_0 + k\varphi_1 + k^2\varphi_2 + \cdots)\theta_0'$$

$$-ik(T_0 + kT_1 + k^2T_2 + \cdots)w_0(x)$$
$$-\eta\left(\varphi'_0 + k\varphi'_1 + k^2\varphi'_2 + \cdots\right) = 0 \quad (23)$$

$$Sc^{-1}\left(\frac{\partial^2}{\partial x^2} - k^2\right)(F_0 + kF_1 + k^2F_2 + \cdots)$$
$$-ik(\varphi_0 + k\varphi_1 + k^2\varphi_2 + \cdots)C'_0$$
$$-ik(F_0 + kF_1 + k^2F_2 + \cdots)w_0(x)$$
$$-(\sigma_0 + k\sigma_1 + k^2\sigma_2 + \cdots)(F_0 + kF_1 + k^2F_2 + \cdots)$$
$$-\eta_c\left(\varphi'_0 + k\varphi'_1 + k^2\varphi'_2 + \cdots\right) = 0 \quad (24)$$

And the boundary conditions are given by

$$\varphi = \varphi_0 + k\varphi_1 + k^2\varphi_2 + \cdots = 0 \; at \; x = \pm 1$$
$$\varphi' = \varphi'_0 + k\varphi'_1 + k^2\varphi'_2 + \cdots = 0 \; at \; x = \pm 1$$
$$\theta' = T'_0 + kT'_1 + k^2T'_2 + \cdots = 0 \; at \; x = \pm 1$$
$$C' = F'_0 + kF'_1 + k^2F'_2 + \cdots = 0 \; at \; x = \pm 1 \quad (25)$$

Collecting various order of k, the equations governing the velocity and temperature perturbations are given by

$$\frac{\sigma_0}{Sc\,Pr}\frac{d^4\varphi_0}{dx^4} - \sigma_0^2\left(\frac{1}{Sc} + \frac{1}{Pr}\right)\frac{d^2\varphi_0}{dx^2} + \sigma_0^3\varphi_0 + \frac{Gr\cos\alpha\,\eta}{Sc}\frac{d^2\varphi_0}{dx^2} + \frac{Gm\cos\alpha\,\eta_c}{Pr}\frac{d^2\varphi_0}{dx^2}$$
$$-\sigma_0 Gr\cos\alpha\,\eta\varphi_0 - \sigma_0 Gm\cos\alpha\,\eta_c\varphi_0 = 0 \quad (26)$$

$$\frac{1}{Pr}\frac{d^2T_0}{dx^2} - \sigma_0 T_0 = \eta\frac{d\varphi_0}{dx} \quad (27)$$

$$\frac{1}{Sc}\frac{d^2F_0}{dx^2} - \sigma_0 F_0 = \eta_c\frac{d\varphi_0}{dx} \quad (28)$$

The qualitative behaviour of eigen value and eigen vector are found to be the same. Hence, we get,

$$\varphi_0 = \cosh R_1 x + A_2\cosh R_2 x$$

$$F_0(x) = A_4\sinh\sqrt{Sc\,\sigma_0}\,x + \eta_c Sc\frac{R_1}{R_1^2 - Sc\sigma_0}\sinh(R_1x) + \eta_c Sc\frac{R_2}{R_2^2 - Sc\sigma_0}\sinh(R_2x)$$

$$T_0(x) = A_5\sinh\sqrt{Pr\,\sigma_0}\,x + \eta\,Pr\frac{1}{R_1^2 - Pr\sigma_0}\sinh(R_1x) + \eta Pr\frac{R_2}{R_2^2 - Sc\sigma_0}\sinh(R_2x)$$

$$\varphi_1(x) = A_5\cosh(R_1x) + A_6\cosh(R_2x) - \sigma_1\{B_7x\sinh(R_1x) + B_8x\sinh(R_2x) + B_9\cosh\sqrt{Pr\sigma_0}\,x + B_{10}\cosh\sqrt{Sc\sigma_0}\,x\} + B_{13}\cosh\left((\lambda + R_1)x\right)$$
$$+B_{14}\cosh\left((\lambda - R_1)x\right) + B_{15}\cosh\left((\lambda + R_2)x\right) + B_{16}\cosh\left((\lambda - R_2)x\right)$$

Imposing the boundary conditions $\phi_1(\pm 1) = 0$ gives the value of σ_1 as

$$\sigma_1 = -\frac{B_{22}}{B_{21}} \quad (29)$$

For brevity, the constants are given in *Appendix.*

4 RESULTS AND DISCUSSION

The present study examines the variation of the growth rate parameter, σ, with respect to key non-dimensional parameters, namely the Prandtl number (Pr), thermal Grashof number (Gr), solutal Grashof number (Gm), Schmidt number (Sc), and the parameter α, in the presence of k the wave number. We have taken the wave number as the control parameter. The graphical results reveal distinct linear and nonlinear influences of these parameters on the system stability.

Figure (1) – (5) shows the influence of the key parameters on the frequency of the disturbances. The variation of σ with *Pr* and k demonstrates a mildly nonlinear dependence. An increase in the Prandtl number results in a gradual enhancement of σ, indicating that fluids with higher momentum diffusivity relative to thermal diffusivity tend to promote instability. However, the curvature of the surface remains weak, suggesting that *Pr* exerts only a moderate influence on the growth characteristics. The parameter k introduces a slight stabilizing tendency, as evidenced by a marginal decrease in σ with increasing k.

In contrast, the dependence of σ on the solutal Grashof number Gm is predominantly linear. The planar nature of the response surface indicates that the contribution of solutal buoyancy forces to instability is directly proportional and does not introduce significant nonlinear effects. This suggests that mass transfer-induced buoyancy acts as a predictable driving mechanism in the system without triggering critical transitions or bifurcations.

A markedly different behaviour is observed in the case of the thermal Grashof number Gr. The nonlinear variation of σ with Gr highlights the dominant role of thermal buoyancy in governing the system dynamics. As Gr increases, σ exhibits a rapid and nonlinear rise, indicating the onset and amplification of convective instability. This behaviour is consistent with classical convection theory, where thermal buoyancy forces drive the transition from stable to unstable regimes.

The parameter α exhibits a nearly linear relationship with σ, as indicated by the planar response surface. The weak sensitivity of σ to α suggests that this parameter acts primarily as a secondary modifier rather than a dominant driver of instability. Its influence appears to be uniform

across the range of k, without introducing any significant interaction effects.

The most pronounced nonlinear behaviour is observed in the variation of σ with the Schmidt number Sc. The strong curvature of the response surface indicates a high sensitivity of the system to changes in Sc. As Sc increases, σ rises significantly, implying that reduced mass diffusivity enhances concentration gradients, thereby intensifying solute convection and instability. This highlights the critical role of mass transport mechanisms in the overall stability characteristics of the flow.

A comparative assessment of all parameters reveals that Gr and Sc are the most influential in determining the growth rate, owing to their strong nonlinear contributions. The Prandtl number exhibits a moderate effect, while Gm and α display largely linear and less dominant influences. The parameter k consistently introduces a mild stabilizing effect across all cases, suggesting its role as a damping or control parameter.

Overall, the results indicate that the instability of the system is governed by a coupled thermo-solute mechanism, wherein thermal and concentration gradients interact to drive convective motion. The nonlinear dependence on Gr and Sc underscores the importance of buoyancy-driven effects, while the linear behaviour associated with Gm and α reflects secondary modulation. These findings provide valuable insight into the relative significance of transport properties and buoyancy forces in determining the stability of electrically conducting or thermally driven shear flows.

We observed from Figures (6)- (11), the variation of σ with the Prandtl number exhibits a weakly nonlinear trend. As Pr increases, σ shows a gradual rise before approaching a near-saturation regime. This behaviour indicates that an increase in momentum diffusivity relative to thermal diffusivity enhances the growth rate, although the effect remains moderate. The limited curvature of the surface suggests that thermal diffusion does not dominate the instability mechanism but rather acts as a secondary contributor. The parameter k consistently introduces a slight reduction in σ, implying a stabilizing influence across the entire parameter space.

A similar stabilizing role of k is observed in all parameter combinations, confirming its function as a damping or control parameter in the system. Its influence is relatively uniform and does not introduce significant nonlinear interactions, indicating that it primarily shifts the baseline of σ without altering the fundamental nature of the instability.

The dependence of σ on the solute Grashof number Gm is found to be predominantly linear. The planar nature of the corresponding response surface indicates that the contribution of concentration-induced buoyancy is directly proportional to Gm. This linearity suggests that solute effects do not trigger abrupt transitions but instead provide a steady and predictable enhancement to the growth rate. Such behaviour is characteristic of systems where mass transfer acts as a supplementary driving force rather than a primary instability mechanism.

In contrast, the thermal Grashof number Gr exhibits a strong nonlinear influence on σ. The response surface demonstrates a pronounced curvature, with σ increasing rapidly as Gr increases. This nonlinear growth reflects the dominant role of thermal buoyancy in driving convective instability. The results are consistent with classical hydrodynamic stability theory, where thermal gradients lead to the onset of convection and significantly amplify disturbance growth rates. The sensitivity of σ to Gr highlights the critical importance of temperature-induced density variations in the system.

The parameter α shows a nearly linear relationship with σ, similar to that observed for Gm. The weak dependence indicates that α functions primarily as a geometric or secondary physical parameter, modulating the growth rate without introducing significant nonlinear effects. Its influence remains consistent across different values of k, further reinforcing its role as a minor controlling parameter.

The Schmidt number Sc demonstrates the most pronounced nonlinear effect among all parameters considered. The response surface exhibits strong curvature, with σ increasing significantly as Sc increases. This behaviour indicates that reduced mass diffusivity enhances concentration gradients, thereby intensifying solutal convection and instability. The high sensitivity of σ to Sc underscores the importance of mass transport processes in determining the overall stability characteristics. In regimes of large Sc, the system becomes increasingly susceptible to instability due to the persistence of concentration gradients.

A comparative analysis of all parameters reveals that the instability mechanism is primarily governed by the combined effects of thermal and solutal buoyancy forces. The parameters Gr and Sc emerge as the dominant contributors due to their strong nonlinear influence on σ. The Prandtl number plays a secondary role, while Gm and α exhibit largely linear and less significant effects. The control parameter k consistently acts to suppress instability, indicating its potential utility in regulating flow behaviour.

Overall, the results demonstrate that the system exhibits a coupled thermo-solute instability, where the interplay between temperature and concentration gradients governs the growth of disturbances. The nonlinear dependence on Gr and Sc highlights the critical thresholds associated with buoyancy-driven convection, while the linear contributions from Gm and α provide steady modulation.

The graphical results presented in figures (12) –(22) illustrate the variation of the stream function φ with respect to selected non-dimensional parameters in the presence of the control parameter k. The response surface

provides insight into the relative sensitivity of the system and the nature of the underlying instability mechanisms.

The variation of φ with respect to the governing parameters exhibits a combination of linear and nonlinear trends, depending on the specific parameter under consideration. In general, the response surfaces indicate that φ is moderately influenced by the control parameter k, which consistently acts to reduce the growth rate. This behavior suggests that k retards the velocity of the disturbances across the parameter space.

For parameters exhibiting linear trends, the corresponding response surfaces are nearly planar, indicating a proportional relationship with the stream function. Such behaviour implies that these parameters contribute in a predictable and steady manner to the instability mechanism, without inducing significant interaction effects or nonlinear amplification. The absence of curvature further suggests that their influence remains uniform across different values of k, reinforcing their role as secondary modifiers of the system dynamics.

In contrast, certain parameters demonstrate a distinctly nonlinear relationship with φ, as evidenced by the curvature of the response surfaces. In these cases, φ increases more rapidly with the parameter, indicating heightened sensitivity and the potential for strong instability. The nonlinear behavior reflects the presence of underlying buoyancy or diffusive mechanisms that intensify as the parameter increases. This is the key characteristic of thermo-solutal systems, where gradients in temperature or concentration can lead to enhanced convective motion and rapid growth of disturbances.

The interplay between linear and nonlinear effects highlights the complexity of the system. While some parameters provide a steady contribution to the growth rate and stream function, others dominate the instability process through nonlinear amplification. The combined effect of these parameters determines the overall stability characteristics, with the nonlinear contributors playing a decisive role in the onset and development of instability.

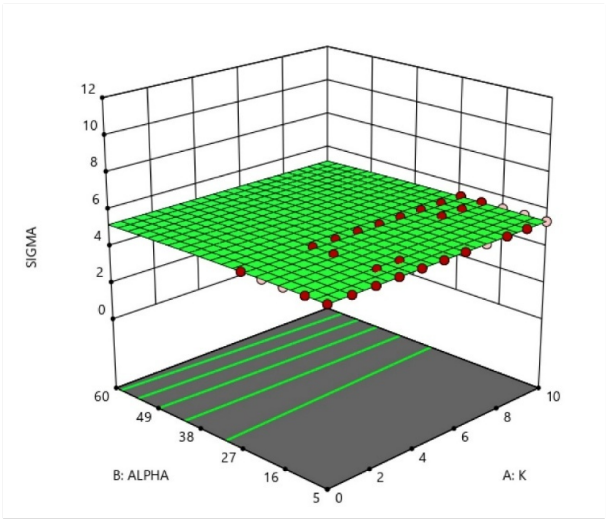

Figure 1. *k vs Alpha vs Sigma*

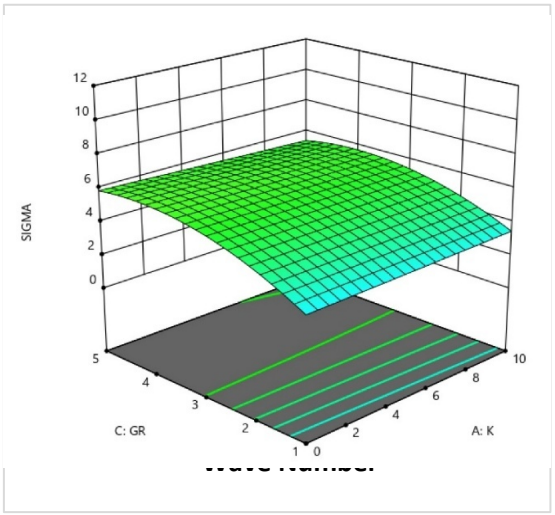

Figure 2. *k vs Gr vs Sigma*

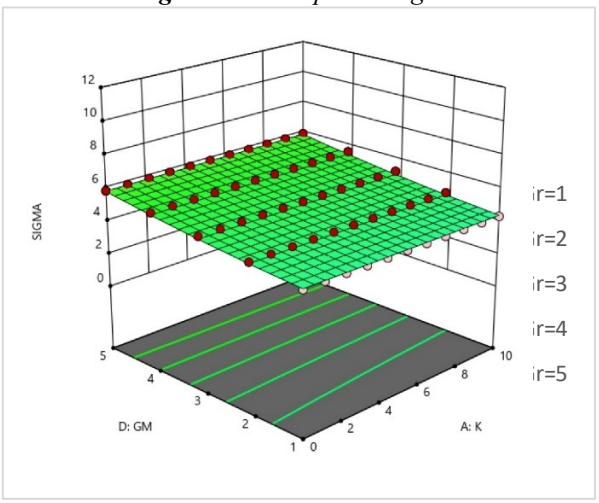

Figure 3. *k vs Gm vs Sigma*

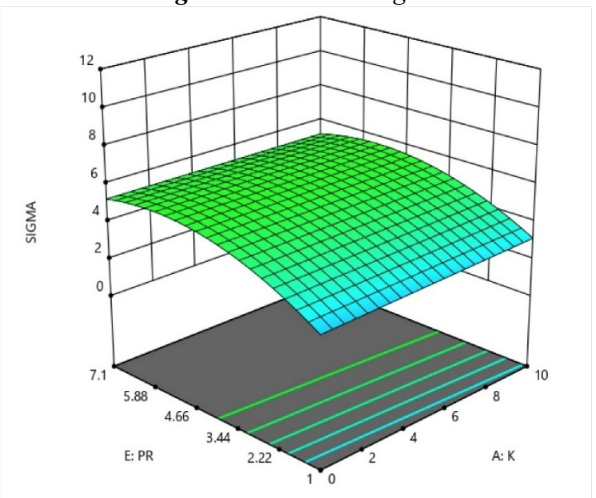

Figure 4. *k vs Pr vs Sigma*

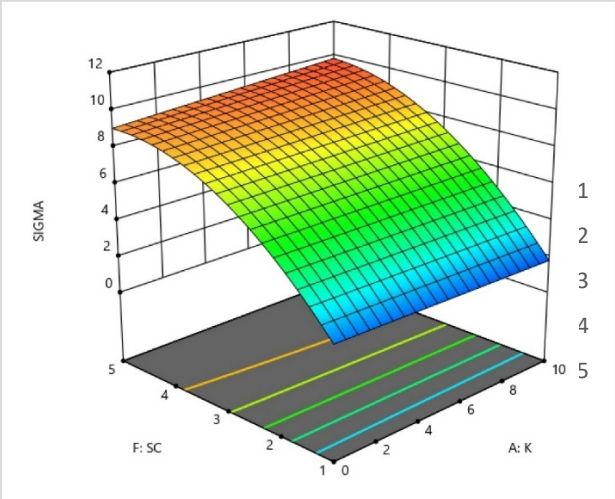

Figure 5.- *k vs Sc vs Sigma*

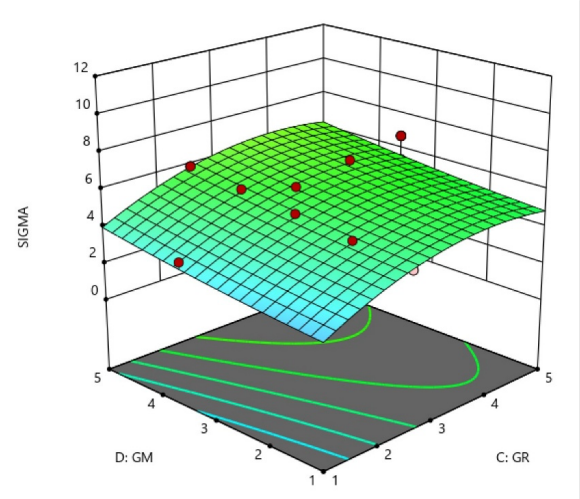

Figure 6.- *Gr vs Gm vs Sigma*

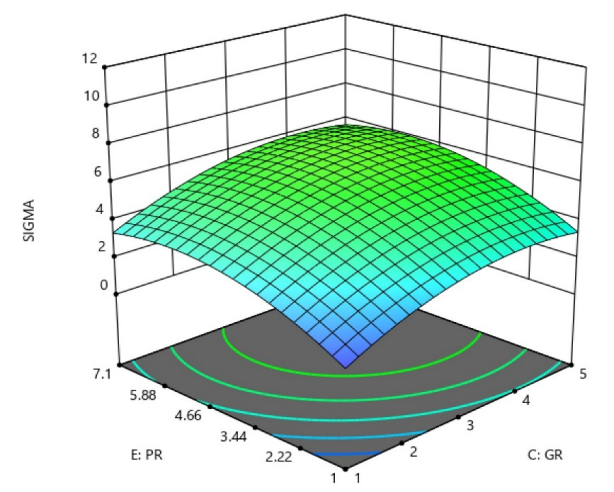

Figure 7. *Gr vs Pr vs Sigma*

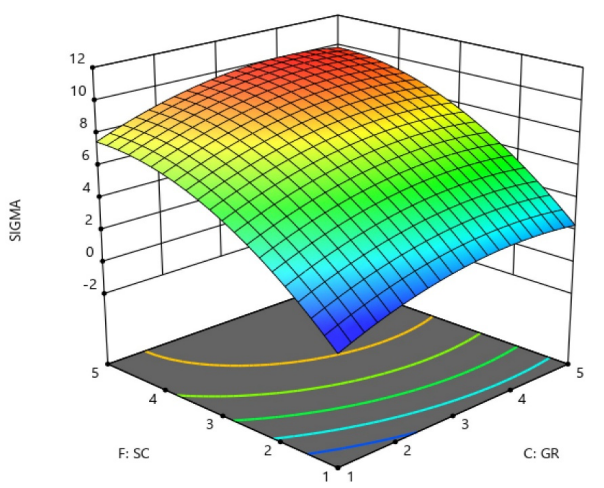

Figure 8. *Gr vs Sc vs Sigma*

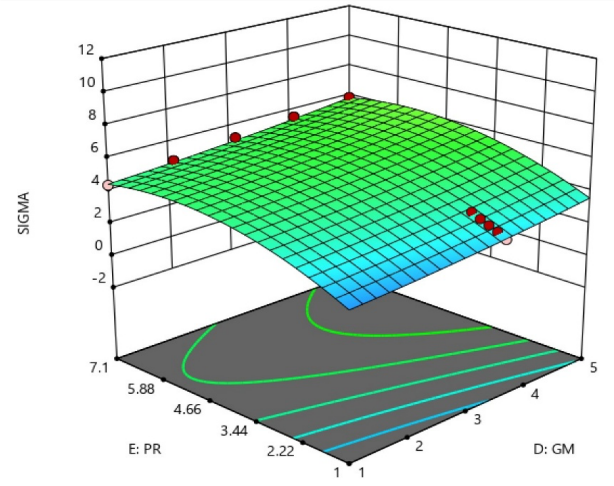

Figure 9. *Gm vs Pr vs Sigma*

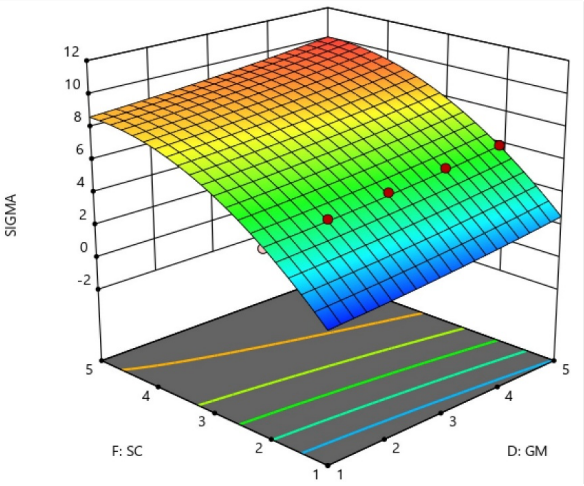

Figure 10 . *Gm vs Sc vs Sigma*

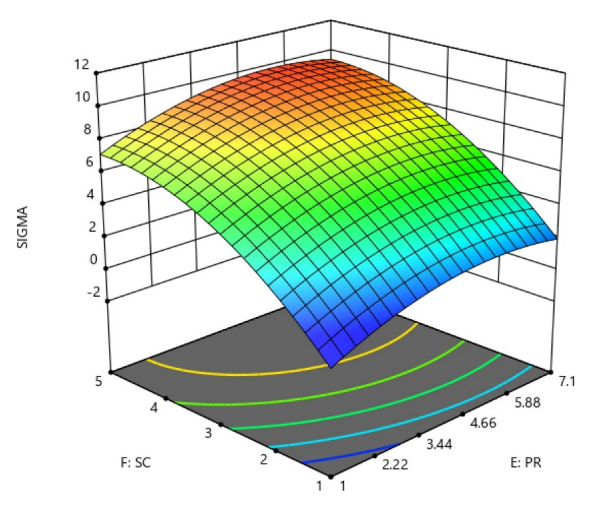

Figure 11. Pr vs Sc vs Sigma

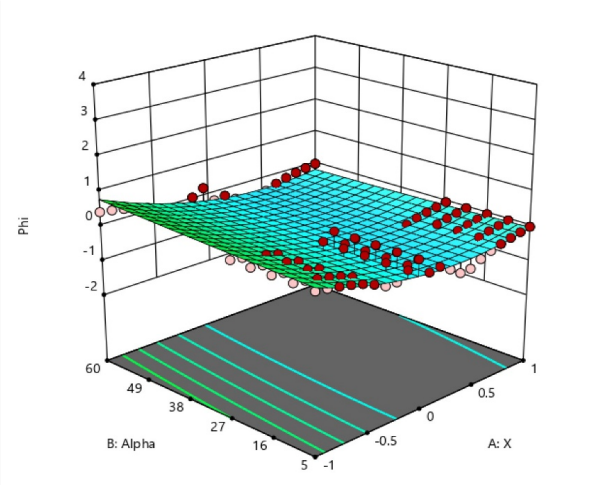

Figure 12. X vs Alpha vs Phi

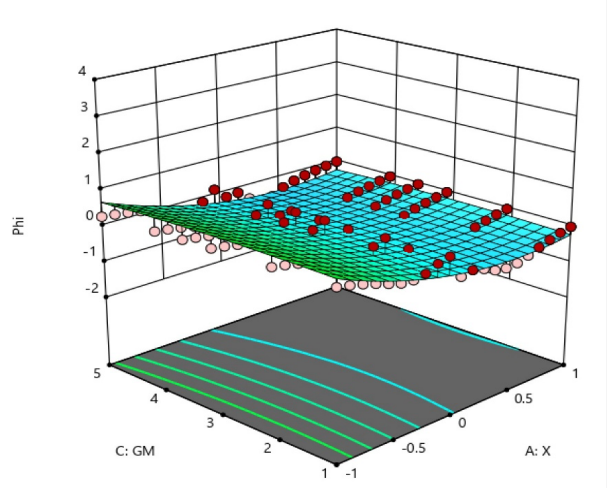

Figure 13.- *X vs Gm vs Phi*

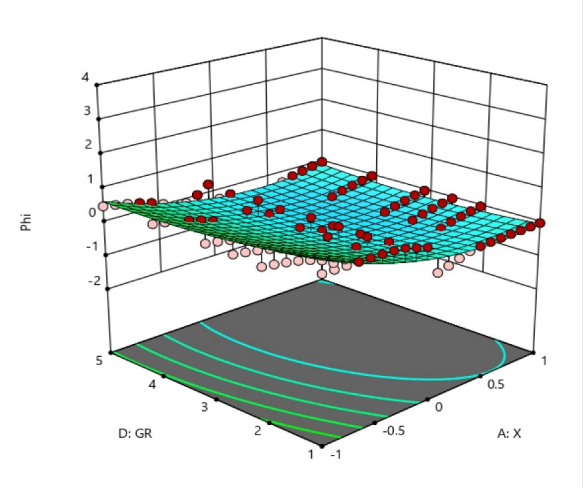

Figure 14 . *X vs Gr vs Phi*

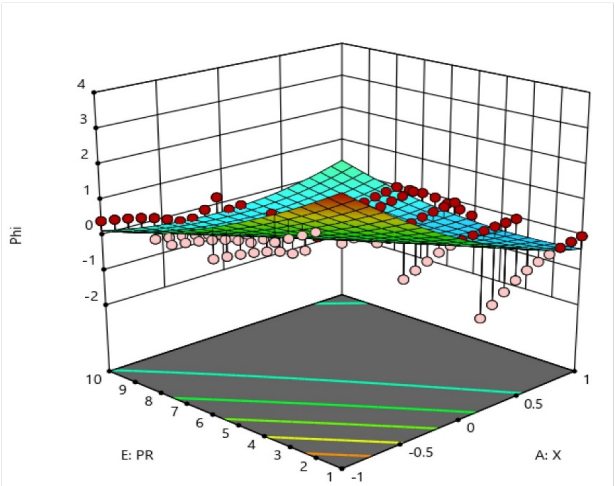

Figure 15. X vs Pr vs Phi

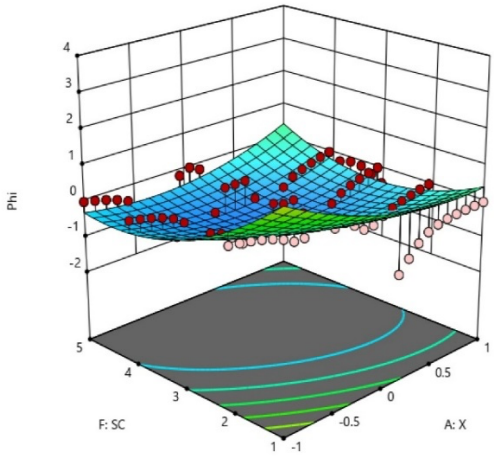

Figure 16. X vs Sc vs Phi

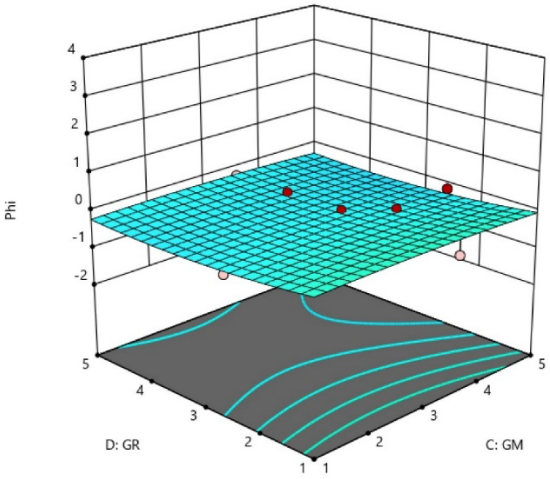

Figure 17. *Gm vs Gr vs Phi*

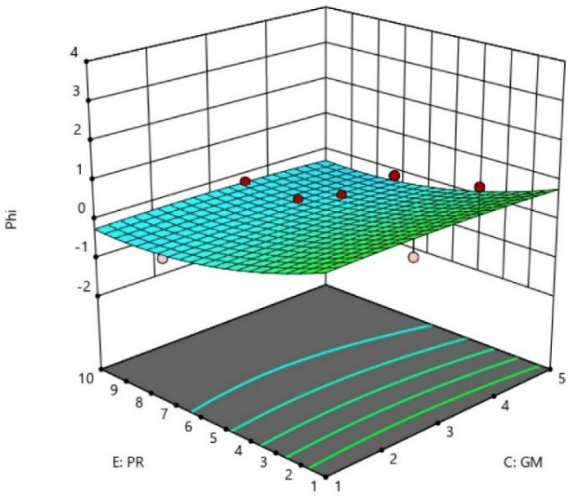

Figure 18. *Gm vs Pr vs Phi*

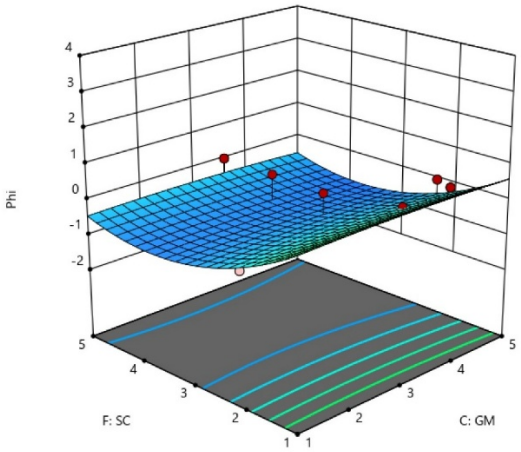

Figure 19. *Gm vs Sc vs Phi*

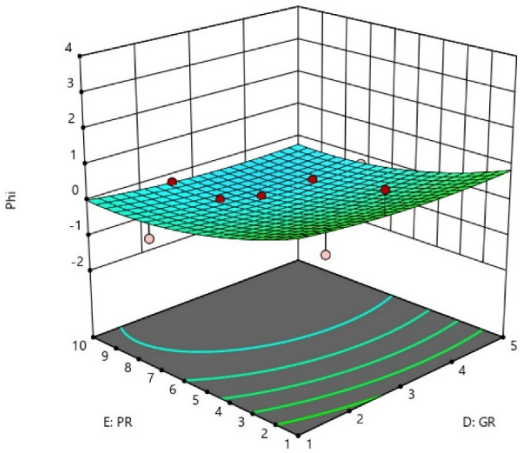

Figure 20. *Gr vs Pr vs Phi*

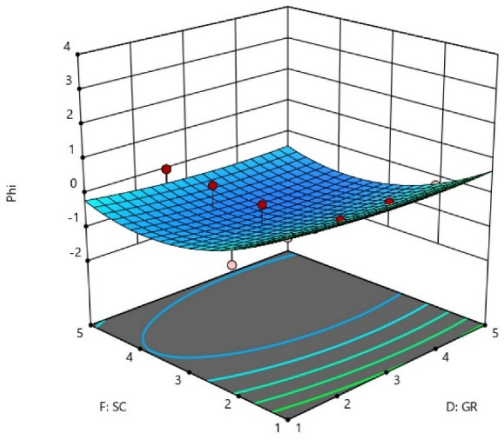

Figure 21. *Gr vs Sc vs Phi*

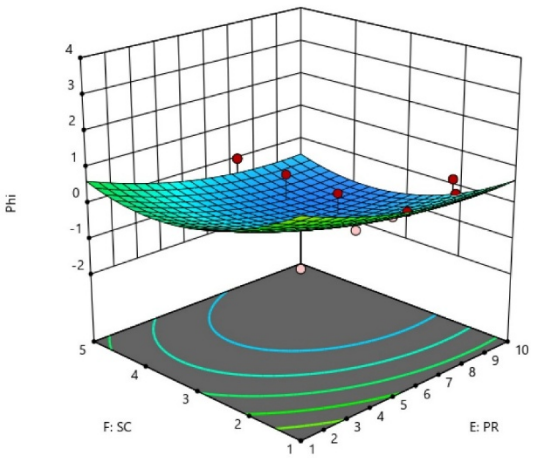

Figure 22. *Pr vs Sc vs Phi*

5 CONCLUSIONS

In this paper we investigated Stability of Double-Diffusive flow in inclined cavities. Analytical expressions are found for the growth rate parameter, σ, with respect to key non-dimensional parameters, namely the Prandtl number (Pr), thermal Grashof number (Gr), solutal Grashof number (Gm), Schmidt number (Sc), and the parameter α, in the presence of K the wave number. We have taken the wave

number as the control parameter. The graphical results reveal distinct linear and nonlinear influences of these parameters on the system stability. Some of the important findings are

- The increase of Prandtl number and alpha is the principal cause of instability as they increase the growth rate of the system.
- The modified Grashof number (Gm) and Schmidt number (Sc) serve to stabilise the system by reducing the growth rate.
- All five parameters studied (α, Pr, Gr, Gm, Sc) have been found to cause a reduction in stream function which implies all have reduced the intensity of the fluid flow.
- The suppression of the stream function demonstrates a consistency between wave number and *x* in the spectral and spatial domain, respectively.

REFERENCES

[1] **Delgado-Buscalioni. R** and **Crespo del Arco. E (1999).** Stability of thermally driven shear flows in long inclined cavities with end-to-end temperature difference*, International Journal of Heat and Mass Transfer,* **42(15), 2811-2822.**

[2] **Gill. A. E. (1966).** The boundary-layer regime for convection in a rectangular cavity, *Journal of Fluid Mechanics*, **26(3), 515–536.**

[3] **Lee. Y** and **Korpela. S. A. (1983).** Multicellular natural convection in a vertical slot, *Journal of Fluid Mechanics*, **126, 91–121.**

[4] **Nield. D.A. (1967).** The thermohaline Rayleigh–Jeffreys problem, *Journal of Fluid Mechanics*, **29(3), 545–558.**

[5] **Sarkar. A** and **Phillips. O. M (1992).** The effects of a vertical stabilizing gradient of solute on the stability of a porous medium, *Journal of Fluid Mechanics*, **240, 1–24**.

[6] **Sharifi. M.,** and **Rasouli. N. (2024).** A comprehensive review of double-diffusive convection in confined geometries: Progress in heat and mass transfer, *International Journal of Thermal Sciences*, **196, Article 108689.**

[7] **Sharifi. M.,** and **Rasouli. N. (2025).** A comprehensive review of double diffusive convection: Effects of flow geometries, external forces, and porous media. *Int. Communications in Heat and Mass Transfer*, **162, 108380**

[8] **Shivakumara. I. S, Rudraiah. N,** and **Narayanan. R (1985)**, The effect of rotation on the linear and non-linear double-diffusive convection in a sparsely packed porous medium, *International Journal of Heat and Mass Transfer*, **28(10),1933–1941.**

[9] **Veronis. G (1968**), Effect of a stabilizing gradient of solute on thermal convection, *Journal of Fluid Mechanics*, **34(2), 315–336.**

[10] **Wood, A.W.** and **Lintz., S.J(1992).** Natural convection and dispersion in a tilted fracture, *J. Fluid Mech*., **241, 59.**

Appendix

$$B_1 = \frac{1}{\mathrm{ScPr}}$$

$$B_2 = \frac{1}{Sc} + \frac{1}{\mathrm{Pr}}$$

$$B_3 = -\frac{\mathrm{Grcos}\ \alpha\eta}{Sc} - \frac{\mathrm{Gmcos}\ \alpha\eta_c}{Pr}$$

$$B_4 = Gr\cos\alpha\eta + \mathrm{Gmcos}\alpha\eta_c$$

$$\sigma_0 = \frac{\left\{-(B_2B_3 - 2B_1B_4) - \sqrt{(B_2B_3 - 2B_1B_4)^2 - 4B_2^2B_3^2}\right\}^{1/2}}{B_2^2}$$

$$A_2 = -\frac{\cosh\ R_1}{\cosh\ R_2}$$

$$\varphi_0(x) = \cosh\,(R_1x) + A_2\cosh\,(R_2x)$$

$$B_5 = -\eta_c Sc\frac{R_1^2}{R_1^2 - Sc\sigma_0}\cosh R_1 - \eta_c Sc\ \frac{R_2^2}{R_2^2 - Sc\sigma_0}\cosh R_1$$

$$A_4 = \frac{B_5}{\cosh\,(\sqrt{\mathrm{Sc}\sigma_0})}$$

$$F_0(x) = A_4\sinh\sqrt{Sc\ \sigma_0}\,x + \eta_c Sc\frac{R_1}{R_1^2 - Sc\sigma_0}\sinh(R_1x) + \eta_c Sc\ \frac{R_2}{R_2^2 - Sc\sigma_0}\sinh(R_2x)$$

$$A_5 = \frac{B_6}{\cosh\,(\sqrt{\mathrm{Pr}\sigma_0})}$$

$$T_0(x) = A_5\sinh\sqrt{Pr\ \sigma_0}\,x + \eta\ Pr\frac{1}{R_1^2 - Pr\sigma_0}\sinh(R_1x) + \eta Pr\ \frac{R_2}{R_2^2 - Sc\sigma_0}\sinh(R_2x)$$

$$w_0(x) = \frac{\cosh\,(\lambda x)}{\cosh\ \lambda} - 1$$

$$B_6 = \frac{1}{\cosh\lambda}$$

$$w_0(x) = B_6\cosh\,(\lambda x) - 1$$

$$B_7 = \frac{1}{R_1^2 - R_2^2}\left(\frac{1}{Sc}R_1^2 - \sigma_0\right)\left(\frac{1}{\mathrm{Pr}}R_2^2 - \sigma_0\right)\frac{1}{2R_1} - \mathrm{Grcos}\alpha\left(\frac{1}{\mathrm{Sc}}R_1^2 - \sigma_0\right)\eta\frac{Pr}{R_1^2 - \mathrm{Pr}\sigma_0}\frac{1}{R_1^2 - R_2^2}\frac{1}{2R_1}$$

$$-\mathrm{Gmcos}\alpha\left(\frac{1}{\mathrm{Pr}}R_1^2 - \sigma_0\right)\eta\ \frac{Sc}{R_1^2 - \mathrm{Sc}\sigma_0}\frac{1}{R_2^2 - R_1^2}\frac{1}{2R_1}$$

$$B_8 = \frac{1}{R_2^2 - R_1^2}\left(\frac{1}{Sc}R_2^2 - \sigma_0\right)\left(\frac{1}{\mathrm{Pr}}R_2^2 - \sigma_0\right)\frac{1}{2R_2} - \mathrm{Grcos}\alpha\left(\frac{1}{\mathrm{Sc}}R_2^2 - \sigma_0\right)\eta\frac{Pr}{R_2^2 - \mathrm{Sc}\sigma_0}\frac{1}{R_2^2 - R_1^2}\frac{1}{2R_2}$$

$$-\mathrm{Gmcos}\alpha\left(\frac{1}{\mathrm{Pr}}R_2^2 - \sigma_0\right)\eta_c\frac{Sc}{R_2^2 - \mathrm{Sc}\sigma_0}\frac{1}{R_2^2 - R_1^2}\frac{1}{2R_2}$$

$$B_9 = -Gr\cos\ \alpha\left(\frac{1}{\mathrm{Sc}}\mathrm{Pr}\sigma_0 - \sigma_0\right)\eta A_5\left(\frac{1}{\mathrm{Pr}\sigma_0 - R_1^2}\right)\left(\frac{1}{\mathrm{Pr}\sigma_0 - R_2^2}\right)$$

$$B_{10} = -Gm\cos\ \alpha\left(\frac{1}{\mathrm{Pr}}\mathrm{Sc}\,\sigma_0 - \sigma_0\right)A_4\left(\frac{1}{\mathrm{Sc}\sigma_0 - R_1^2}\right)\left(\frac{1}{\mathrm{Sc}\sigma_0 - R_2^2}\right)$$

$$B_{11} = B_6\lambda^2 - B_6R_1^2$$

$$B_{12} = B_6\lambda^2A_2 - A_2R_2^2B_6$$

$$B_{13} = \frac{B_{11}}{2}\frac{1}{(\lambda + R_1)^2 - R_1^2}\frac{1}{(\lambda + R_1)^2 - R_2^2}$$

$$B_{14} = \frac{B_{11}}{2}\frac{1}{(\lambda - R_1)^2 - R_1^2}\frac{1}{(\lambda - R_1)^2 - R_2^2}$$

$$B_{15} = \frac{B_{11}}{2}\frac{1}{(\lambda + R_2)^2 - R_1^2}\frac{1}{(\lambda + R_2)^2 - R_2^2}$$

$$B_{16} = \frac{B_{11}}{2}\frac{1}{(\lambda - R_2)^2 - R_1^2}\frac{1}{(\lambda - R_2)^2 - R_2^2}$$

$$B_{17} = B_7\sinh(R_1) + B_8\sinh(R_2) + B_9cosh\sqrt{Pr\sigma_0} + B_{10}cosh\sqrt{Sc\sigma_0}$$

$$B_{18} = -\{B_{13}\cosh\,(\lambda + R_1) + +B_{14}\cosh(\lambda - R_1) + B_{15}\cosh(\lambda + R_2) + B_{16}\cosh\,(\lambda - R_2)\}$$

$$B_{19} = B_7(\mathrm{Sinh}(R_1) + R_1\cosh\,(R_1)) + B_8\big(\sinh\,(R_2) + R_2\cosh\,(R_2)\big)$$

$$+\mathrm{B}_9\sqrt{\mathrm{Pr}\sigma_0}\sinh\,(\sqrt{Pr\sigma_0}\,x) + B_{10}\sqrt{Sc\sigma_0}\sinh(\sqrt{Sc\sigma_0}\,x)$$

$$B_{20} = -\{B_{13}(\lambda + R_1)\sinh(\lambda + R_1) + B_{14}\,(\lambda - R_1)\sinh\ (\lambda - R_1) + B_{15}(\lambda + R_2)\sinh(\lambda + R_2) + B_{16}(\lambda - R_2)\sinh(\lambda - R_2)\}$$

$$B_{21} = B_{17}R_1\sin(R_1) - B_{19}\cosh(R_1)$$

$$B_{22} = B_{18}R_1\sin(R_1) - B_{20}\cosh(R_1)$$

$$\sigma_1 = -\frac{B_{22}}{B_{21}}$$

$$A_6 = \frac{\sigma_1B_{17} + B_{18} - \cosh\,(R_1)}{\cosh\,(R_2)}$$

$$\varphi_1(x) = A_5\cosh(R_1x) + A_6\cosh(R_2x) - \sigma_1\{B_7x\sinh(R_1x) + B_8x\sinh(R_2x) + B_9\cosh\sqrt{Pr\sigma_0}\,x + B_{10}\cosh\sqrt{Sc\sigma_0}\,x\} + B_{13}\cosh\big((\lambda + R_1)x\big) + B_{14}\cosh\big((\lambda - R_1)x\big) + B_{15}\cosh\big((\lambda + R_2)x\big) + B_{16}\cosh\big((\lambda - R_2)x\big)$$